FEASIBILITY ANALYSIS OF UNDERGROUND COMPRESSED AIR ENERGY STORAGE IN LINED ROCK CAVERNS USING THE TOUGH-FLAC SIMULATOR

Hyung-Mok Kim[1)], Jonny Rutqvist[2)], Byung-Hee Choi[3)]

[1)] Energy and Mineral Resources Engineering, Sejong University
98 Gunja-Dong, Gwangjin-Gu, Seoul 143-747 Korea
e-mail: hmkim@sejong.ac.kr (H.M. Kim)
[2)] Lawrence Berkeley National Laboratory (LBNL)
1 Cyclotron Rd. Berkeley, CA94720 USA
e-mail: jrutqvist@lbl.gov (J. Rutqvist)
[3)] Korea Institute of Geoscience and Mineral Resources (KIGAM)
124 Gwahang-no, Yuseong-gu, Daejeon 305-350 Korea,
e-mail: bhchoi@kigam.re.kr (B.H. Choi)

ABSTRACT

In this paper, we describe the use of the TOUGH-FLAC simulator for feasibility analysis of underground compressed air energy storage (CAES) within lined rock caverns (LRC). We investigated complex thermodynamic processes involved in the CAES operation, such as heat transfer during the compression and decompression of air, groundwater flow and potential leaked-air migration, and mechanical deformation induced by pressurized air in the storage cavern. For this feasibility study, we conducted a 2-D model simulation of a vertical cross section within an LRC for compressed air storage (up to 8 MPa) at the relatively shallow depth of 100 m. In the model, vital components of the CAES system were incorporated, including the cavern, surrounding rock, an excavation damaged zone (EDZ), a concrete lining, and a thin, impermeable, inner synthetic lining. The simulation results demonstrate that underground CAES in LRCs, even at a shallow depth, can be technically feasible with respect to air tightness, energy efficiency, and geomechanical stability. This model approach will be validated through a planned pilot-scale test in Korea where the proposed underground CAES concept will be studied *in situ*.

INTRODUCTION TO UNDERGROUND CAES IN LINED ROCK CAVERNS

Large-scale energy storage systems (ESS) are becoming more important for load leveling, especially in connection with increasing interest in renewable energy. Wind and solar power are promising energy sources, but they are intermittent, which means that they cannot provide electricity steadily and stably, owing to changing weather conditions. They are also often located at remote distances from the energy demand.

Along with pumped hydroelectric storage, underground compressed air energy storage (CAES) is considered to be one of the most promising large-scale electric-energy-storage technologies. In CAES, excess electric energy is used to compress air, which is then injected into underground caverns, large cavities (in salt deposits or mines) or porous reservoirs (aquifers or depleted hydrocarbon reservoirs). When power demand exceeds supply, compressed air is produced from the cavern or reservoir, and fed into a gas turbine that produces electricity that is provided to the grid (Figure 1).

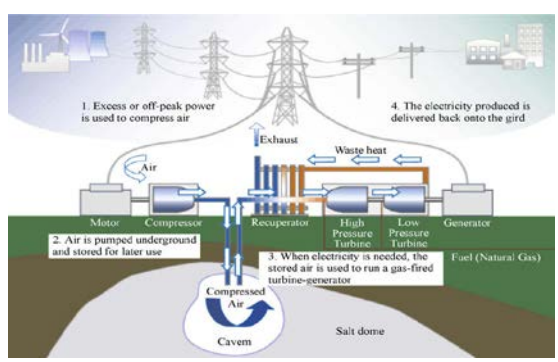

Figure 1. Sketch of an underground CAES reservoir http://www.scotland.gov.uk/, accessed 2012.7).

Excavated underground rock caverns for CAES may be more expensive to develop than solution-mined salt cavities and naturally occurring reservoirs. However, excavation of rock caverns provides more possibilities for site selection closer to energy sources (wind and solar power). Including the transmission-line cost from energy source to demand, the overall costs of energy storage can be reduced by the use of well-located excavated rock caverns. Moreover, CAES in rock caverns lined and reinforced by concrete and steel can be located at shallow depths, independent of surrounding geological conditions, thus significantly reducing construction costs and enabling even greater flexibility in site selection.

THERMODYNAMIC AND GEOMECHANICAL PROCESSES ASSOCIATED WITH UNDERGROUND CAES

General requirements for underground rock caverns for CAES include stability, air tightness, acceptable surface uplift, and eventual environmentally safe decommissioning and abandonment. These general requirements are influenced by thermodynamic and geomechanical design parameters, such as cavern geometry and volume, cavern depth, operation pressure and temperature inside the cavern, distance between the caverns (in case of multiple storage caverns), allowable convergence of the excavated cavern, and operation patterns—in addition to the strength and permeability of concrete linings and surrounding rock mass. Groundwater table level and degrees of saturation in both concrete linings and rock are key in maximizing storage pressure while minimizing air leakage.

Significant temperature changes are expected during the compression and decompression cycles. As a result of such temperature changes and heat transfer to the concrete lining and surrounding rock mass, thermal stresses could be induced that could influence the mechanical stability of a storage cavern. In addition, highly pressurized air may significantly reduce effective stress, which in turn may impact mechanical stability and air leakage.

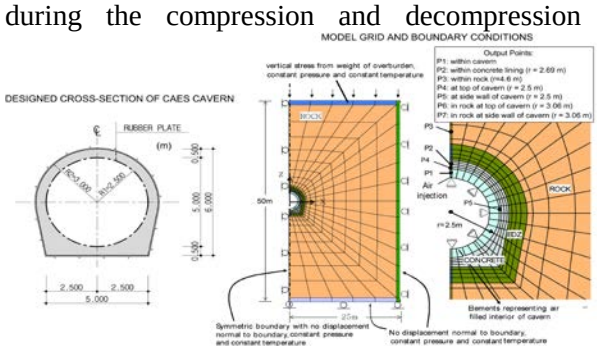

Figure 2. Preliminary design of a cross section of a rock cavern for CAES with concrete lining and model grid with boundary conditions.

ANALYSIS MODEL AND CONDITIONS

We conducted numerical modeling of coupled thermodynamic, multiphase fluid flow, and heat transport associated with underground CAES in lined rock caverns using the TOUGH-FLAC simulator (Rutqvist, 2011). The principles of TOUGH-FLAC coupled analysis are not discussed in detail in this paper. In short, the simulator is based on linking two established codes, TOUGH2 (Pruess et al., 1999) for multiphase flow and heat transfer, and FLAC3D (Itasca, 2009) for geomechanical analysis using sequential coupling and data transfer.

For this study, we carry out a 2-D model simulation for a vertical cross section of an underground CAES system, based on a preliminary design for a pilot test in Korea. The numerical grid shown in Figure 2 contains the vital components of the CAES system, including the cavern, rock, concrete lining, and an excavation disturbed zone (EDZ) that could have different material properties from the surrounding undisturbed host rock. As an option, we could also simulate a thin, impermeable synthetic seal at the inner surface of the concrete lining. In our model, the optional inner-surface synthetic seal is so thin that it has no load-bearing capacity, meaning that the air pressure within the cavern is directly transferred as stress normal to the inner surface of the concrete lining

In the model, the interior of the air-filled cavern is explicitly represented as a medium of high porosity (1.0), high permeability (1.0×10^{-9} m^2), and mechanical softness (E = 3.5 MPa, v = 0.3). The exact values used for the permeability and

deformation modulus of the cavern interior are not important, as long as the values are much less than the values for the concrete lining and surrounding rock. This approach was verified to be useful in simulating air pressure, temperature, and even stress exerted from the air pressure on the inner surface of the lining (Rutqvist el al., 2012). A set of base-case material properties for our analysis is listed in Table 1.

Table 1. Material properties used as a base case for modeling of CAES in a lined rock cavern.

Property	Material		
	Rock mass	EDZ	Concrete lining
Young's modulus, E (GPa)	35	35	35
Poisson's ratio, ν (-)	0.3	0.3	0.3
Thermal expansion coefficient (°C^{-1})	1×10^{-5}	1×10^{-5}	1×10^{-5}
Effective porosity, ϕ (-)	0.01	0.01	0.1
Permeability, k, (m^2)	1×10^{-17}	1×10^{-17}	1×10^{-20}
Residual gas saturation (-)	0.0	0.0	0.0
Residual liquid saturation(-)	0.01	0.01	0.01
van Genuchten, P_0 (MPa)	1.47	1.47	1.47
van Genuchten, m (-)	0.595	0.595	0.595
Thermal conductivity λ (J/s/m K)	3	3	3
Specific heat (J/kg K)	900	900	900

When modeling coupled thermodynamic and geomechanical behavior, we must capture the entire construction and operation sequence. The system therefore was initialized by the following steps:

Step 1: Initial simulation to achieve steady-state vertical gradients of pore pressure, temperature, and stress in the rock mass as initial conditions before excavation.

Step 2: Excavating the cavern and keeping it open for 1 week at atmospheric pressure within the open cavern, to allow the cavern to converge mechanically and to achieve new distributions of pressure, temperature, and stress in the rock mass.

Step 3: Installing the concrete lining at a specific initial saturation (e.g., 70%), atmospheric air pressure, and near-zero effective stress, to keep atmospheric air pressure in the cavern.

After Step 3, proper initial conditions for the start of the CAES operation are achieved. This includes atmospheric cavern pressure, a concrete lining with an initial saturation of 70% and zero stress, a fully saturated surrounding rock mass with excavation induced gradients of pressure, and stress concentrations around the cavern.

After this initialization, the simulated CAES operation was started by injecting and withdrawing air from the cavern for various modeling cases. Analysis conditions are summarized in Table 2.

Table 2. Analysis conditions for initialization and operation simulations.

Initialization
· Cavern depth: 100m
· Rock mass specific weight: 2,700 kg/m^3
· Ground surface temperature: 10 °C
· Vertical gradient of temperature: 0.03 °C/m
· Groundwater table is close to ground surface
· Isotropic stress field (vertical stress equals to overburden rock mass)
Operation
· Operation pressure range: 5 to 8 MPa
· Daily cycle: constant rate injection (8h) - shut in (4h) - constant rate production (4h) - shut in (8h)
· Constant injection rate: 2.2×10^{-2} kg/s
· Constant production rate: 4.2×10^{-2} kg/s
· Injection temperature: 21.5 °C

RESULTS AND DISCUSSION

Base case simulation

We first present an initial model simulation for one daily compression and decompression cycle, which will show the general thermodynamic and mechanical deformation response of the system. Figure 3 shows the calculated evolution of pressure and temperature at three points (P1, within the cavern; P2, within the concrete lining; and P3, within the rock), with their locations shown in Figure 2. Figure 3 also shows the radial displacements of the inner surface of the concrete lining and stress evolution at a point (P2) located in the concrete lining (positive values signify tension). The results show pressure evolution induced by a pre-designed daily cycle of compression and decompression. Some changes in gas pressure and temperature occur in the concrete lining, whereas pressure and temperature do not change significantly in the rock a few meters from the excavation. Figure 3(c) shows that the air-filled cavern expands and contracts with a maximum magnitude of 0.3 mm (radius change). This is a very

small displacement, leading to a volume change of about 5×10^{-3} m^3—negligible compared to the total cavern volume of 19.63 m^3. In Figure 3(d), it is shown that the maximum and minimum compressive effective stresses (taking into account gas pressure evolution) are synchronized with the pressure evolution during the daily cycle.

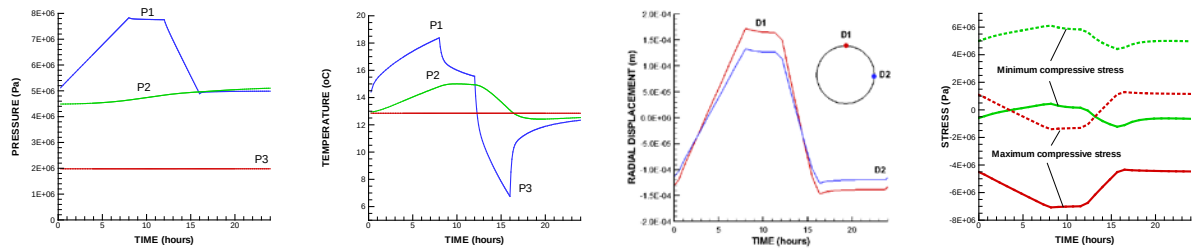

(a) (b) (c) (d)

Figure 3. Calculated evolution of (a) pressure (b) temperature (c) radial displacement of the inner surface of the concrete lining (d) stress in the concrete lining (P2) (green lines are maximum compressive stress, red lines minimum compressive stress; dashed lines are effective stresses and solid lines total stresses)

Air tightness performance

The total mass stored in a storage cavern at a certain pressure and temperature can be estimated from the ideal gas law. During compression and decompression cycles, pressure and temperature within the cavern vary nonlinearly with time, and with the air mass lost from the cavern; a leakage rate can be determined using Eq. (1) according to.

$$\Delta m = m_1 - m_2 = \frac{V_{cavern}}{R_{air}}\left(\frac{P_1}{T_1} - \frac{P_2}{T_2}\right) \qquad (1)$$

where m is mass of gas (kg), P is absolute pressure (Pa) within the cavern, V_{cavern} is cavern volume (m^3), R_{air} is the specific gas constant for air (=286.9 J/kg K), and T is absolute temperature (K). Total volume of the open cavern inside the concrete lining is assumed constant during compression and decompression cycles. Subscripts 1 and 2 indicate initial and later states, respectively.

Figure 4 presents the evolution of leakage rate and daily leakage percentage for various combinations of lining and rock permeability. The results show that leakage of less than 1% would be achieved if permeability of the concrete lining were less than 1×10^{-18} m^2, even if the permeability of the rock were as high as 1×10^{-15} m^2. A less than 1% leakage rate is also achieved if the rock mass permeability were less than 1×10^{-17} m^2, even with a comparatively permeable concrete lining.

Figure 5 presents the leakage rate and daily leakage percentage as a function of gas saturation in the lining, when the lining intrinsic permeability is 1×10^{-16} m^2, i.e. a relatively high value. The leakage rate increases with increasing gas saturation (decreasing water saturation) in the concrete lining, indicating that the saturation in the concrete has a significant impact on the CAES system air tightness. We calculated a daily leakage of 12% when the gas saturation in the concrete lining was 74%, while the leakage rate decreased to 0.8% when the gas saturation was 29%. Our simulations indicate that a daily leakage of 12% would be achieved as the lining dries out after 3 years of continuous operation. Thus, unless the gas saturation of the lining can be kept low, a lining permeability of 1×10^{-16} m^2 does not provide sufficient air-tightness for an efficient CAES system.

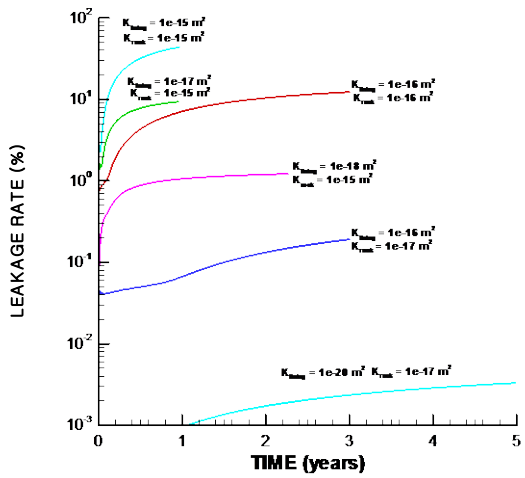

Figure 4. Calculated evolution of daily leakage percentage for different combinations of concrete lining and rock permeability

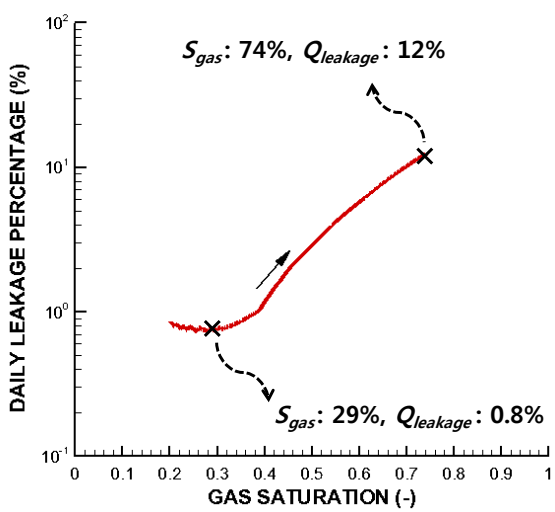

Figure 5. Calculated daily leakage percentage versus saturation in the concrete lining for a lining intrinsic permeability 1×10^{-16} m^2.

Thermodynamic energy efficiency

The energy balance equation for the CAES system can be written as follows (Kim et al., 2012):

$$C_{air}T_s\Delta m_s = \frac{C_{air}}{R}V_s\frac{\partial P_s}{\partial t} = (C_{air}+R_{air})T_m\Delta m_m - (C_{air}+R_{air})T_l\Delta m_l + (\Delta Q_c + \Delta Q_a) \quad (2)$$

where Δm_s is the rate of change of stored air mass, m_m and m_l are the mass flows (kg/s) by air movement due to injection and production as well as air leakage, and air is assumed to be an ideal gas. T_s, T_m, and T_l are the temperatures (K) of stored air, injected/produced, and leaking air, respectively. Here, V_s is the volume of stored air, equal to cavern volume. T_m is equal both to the injection temperature (21° C = 294.15 K) during compression and to cavern temperature, i.e., the temperature of stored air T_s during decompression. The temperature of leaking air (T_l) is taken to be equal to the temperature of stored air (T_s). C_{air} is the specific heat of air at constant volume (1,006 J/(kg K)), and R_{air} is the specific gas constant for air (286.9 J/(kg K).

Eq. (2) indicates that the change in total energy stored in the CAES underground cavern can be expressed as the summation of the internal energy change, the work done by injected compressed air, and the sum of outflows from production, air leakage, and heat transfer. From the TOUGH2 simulation, each term of the above energy balance equation was evaluated.

Figure 6 demonstrates the energy loss and gain for a tight and leaky case including both air leakage and heat transfer, with a negative energy rate indicating an energy gain. The shaded area in Figure 6(b) represents the energy loss solely by air leakage; air leakage and consequent energy loss are clearly more significant in leaky lining cases with higher permeability of concrete linings.

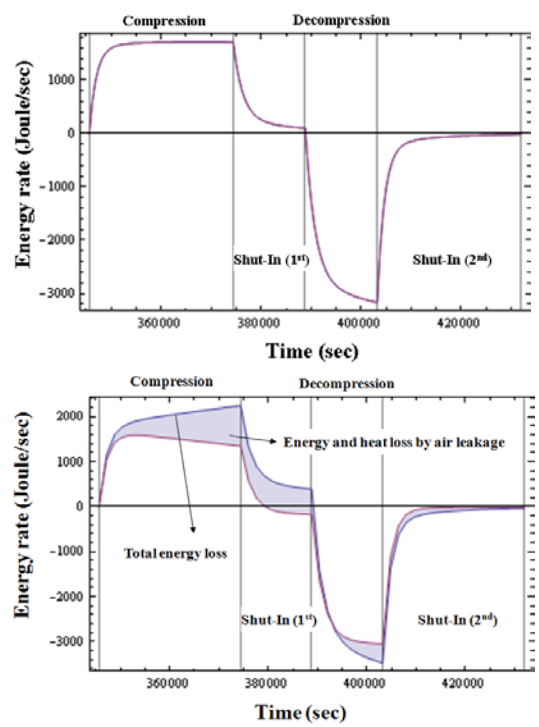

Figure 6. Energy balance analysis for (a) tight lining case with concrete lining permeability of 1.0 x 10^{-18} m^2, (b) leaky lining case with concrete lining permeability of 1.0 x 10^{-16} m^2

For a more quantitative energy-balance analysis, we calculated the time-integrated values for each term in Eq.(2). In the tight-lining case, the energy loss through heat conduction was greater than that through air leakage by two orders of magnitude, constituting as much as 28% of the total injected energy during compression. Energy gain—the energy recovered through heat conduction from the concrete lining to the stored air during the decompression phase— was as much as 24% of total injected energy. Thus, 4% of injected energy was lost during the cycle. In the leaky lining case, total energy loss during the compression phase was as much as 36% of total injected energy, and ultimately 10% of the total injected energy was lost due to air leakage.

We also investigated the influence of injection temperature and the thermal conductivity of the concrete lining on energy balance. We found that the energy loss from heat conduction can be minimized by keeping the air-injection temperature closer to the ambient temperature of the storage cavern. (The thermal conductivity of the concrete linings was insignificant.)

Geomechanical stability

Coupled modeling to study the geomechanical stability of the underground CAES system was conducted in several steps to simulate the sequence of excavation, installation of concrete lining, and subsequent air compression from an initial atmospheric pressure to CAES operation pressure. In this simulation, we assumed that the concrete lining is installed several months after excavation. The initial pressure in the cavern is atmospheric and the initial stress in the concrete lining is zero. The initial water saturation within the concrete lining is 70%, and the rock mass outside the concrete lining is fully saturated.

Figure 7 presents the results of pressure and stress in the concrete lining during a simulation over 100 daily cycles. Figure 7(a) shows the results for a simulation case assuming that the concrete lining serves as a primary seal with a relatively low permeability of 1.0 × 10^{-20} m^2. On the other hand, Figure 7(b) shows the simulation results for a case in which a perfect synthetic air-tight seal (e.g. welded steel lining or rubber sheet) is installed inside the concrete lining.

In Figure 7, we also show, in more detail, the results for the first 7 cycles (first week) as well as one cycle at the end of the 100-day simulation (cycle#100). For the case of concrete lining as a primary seal, the pore pressure in the concrete lining (P2 in Figure 7(a)) increases slowly with time and reaches about 6 MPa by the end of the 100th cycle. This pressure increase has implications for the mechanical stability of the CAES system, since it leads to changes in the effective stress in the concrete lining. Figure 7 further shows the evolution of maximum and minimum principal stresses. Red lines are total stresses; green lines are effective stresses. Most importantly, the minimum principal stress is in tension (positive sign), and the tension increases over time in concert with the increase in gas pressure within the lining. In Figure 7(a), at the 100th day, the minimum effective principal stress fluctuates between 5 to 7 MPa (tensile stress), which may initiate radial fractures and air leakage through the fractures.

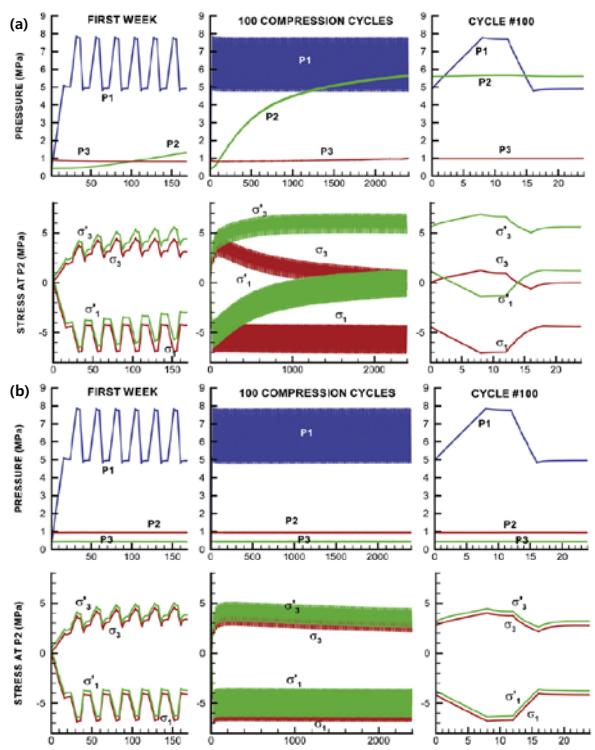

Figure 7. Calculated pressure and stress in the concrete linings during the 100 cycles, (a)

when only the concrete lining was installed, (b) when the air-tight inner seal was installed inside the concrete lining.

The main difference between the case with the impermeable internal seal (Figure 7(b)) and the case without internal seal (Figure 7(a)), is that in the former, the fluid pressure within the concrete lining remains constant and equal to the initial pressure. As a result, the minimum effective principal stress does not exceed 5 MPa in tension over the entire 100-day simulation time. This shows that an impermeable synthetic seal can help to reduce effective tensile stress, and reduce the potential for fracturing in the concrete lining.

The potential impact of permeability changes in the concrete lining as a result of straining and potential fracturing was investigated. Laboratory data showed that cracked concrete is several orders of magnitude more permeable than intact, uncracked concrete (Hoseini et al., 2009). Laboratory results have also indicated a threshold in the crack-opening displacement (COD), below which there is no significant change in permeability. In this study, we estimated COD from the tangential strain, assuming that when tensile failure occurs, the tangential strain is localized to opening of one fracture intersecting the element. We related the COD (equivalent to aperture) to permeability using the cubic law for fracture flow, and then calculated the change in equivalent permeability resulting from crack opening, as if it were superimposed on the initial rock permeability (Figure 8).

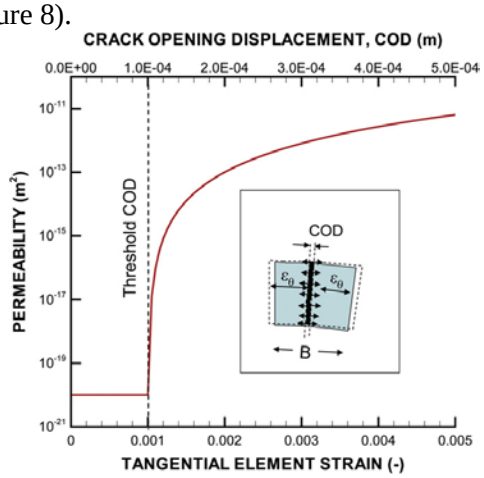

Figure 8. Element strain (and implicit crack opening displacement) versus element permeability model for simulating permeability changes caused by cracking of concrete lining (Rutqvist et al., 2012).

Figures 9 and 10 show how pressurization of a cavern leads to tensile failure and localized permeability increases, and a breakthrough, with air leakage out of the cavern. The modeling results showed that larger strains are localized at the top of the cavern and at one location at the side of the cavern after 24 hours. At this instant, the air pressure quickly propagates through the concrete lining and leads to an increase in pressure within the rock mass outside the lining. However, despite an abrupt pressure change in the lining and in the surrounding rock mass, the average pressure within the cavern remains nearly constant during 10 cycles of simulation, indicating that fracturing within the concrete lining has no significant impact on the pressure evolution within the cavern. We also investigated the influence of the excavation damaged zone (EDZ) on the geomechanical performance of CAES in lined rock caverns.

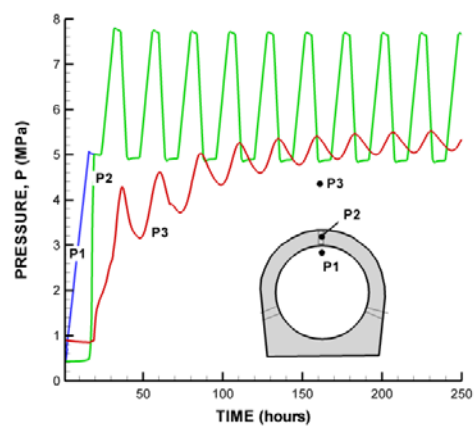

Figure 9. Calculated evolution of pressure through a tensile crack in concrete linings during 10 pressure cycles using the element strain versus permeability function.

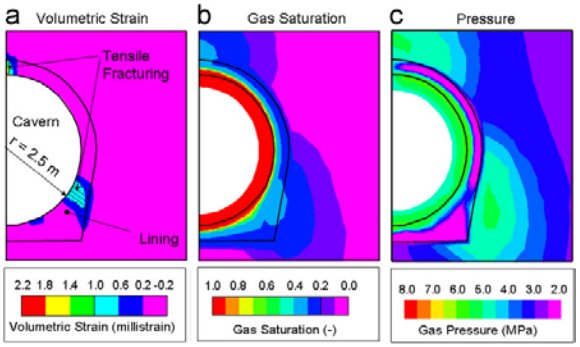

Figure 10. Calculated distribution of (a) volumetric strain, (b) saturation, and (c) pressure after 10 pressure cycles when cracking has occurred in the concrete lining.

Figure 11 compares the calculated evolution of stress within the concrete lining and the radial displacement of the inner surface of the concrete lining under more or less compliant EDZ conditions. Here, the compliance of the EDZ was defined as EDZ thickness multiplied by EDZ compressibility. In Figure 11, the increased compliance of the lining-EDZ-rock system results in an increase of tangential stress from 2.4 to 5.26 MPa, and radial displacement from 0.46 to 0.66 mm. From our further simulations, aiming at more precisely investigating the relative effect of the EDZ on the concrete lining, we found that the most favorable design for reducing tensile tangential stress in the lining would be a relatively compliant lining and relatively stiff (uncompliant) rock that is not significantly softened in the EDZ.

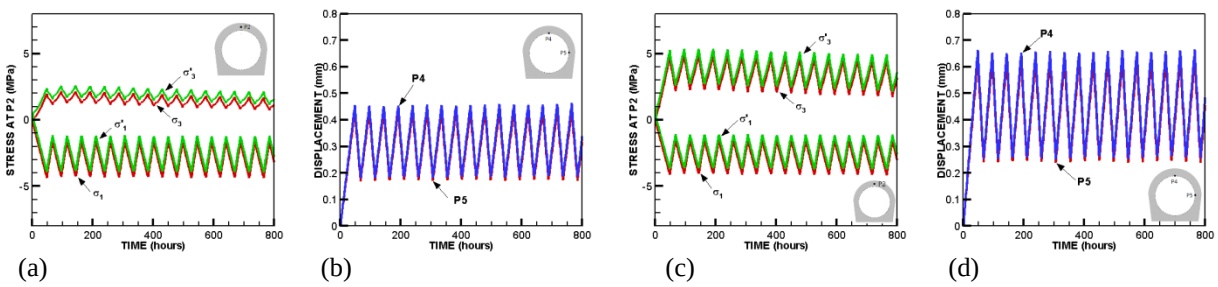

Figure 11. Calculated evolution of (a) stress and (b) displacement of concrete lining in less compliant EDZ condition, and (c) stress and (d) displacement of concrete lining in more compliant EDZ condition.

SUMMARY AND CONCLUSIONS

We carried out numerical modeling of coupled thermodynamic, multiphase fluid flow and geomechanical processes associated with underground CAES in a lined rock cavern. Specifically, we investigated air tightness, energy efficiency, and the geomechanical stability.

Our air-mass balance analysis showed that the key parameters for assuring the long-term air tightness of the CAES system were (1) the permeability of both the concrete lining and the surrounding rock and (2) the gas (and water) saturation of the lining. The analysis shows that the concrete lining would dry out over time, leading to increased leakage, unless the concrete can be kept moist at a relatively high liquid saturation. Nevertheless, a concrete lining with a permeability of less than 1×10^{-18} m^2 would result in an acceptable air-leakage rate even if completely dry. Subsequent energy-balance analyses demonstrated that the energy loss for a daily compression and decompression cycle depends on the air-pressure loss, as well as on energy loss resulting from heat conduction to the concrete lining and surrounding rock. In our geomechanical analysis, investigating the potential failure from tensile stress in concrete linings, we found that the air leakage out of a cavern did not increase to unacceptable levels even after a significant pressure increase in the surrounding rock—as long as the rock is sufficiently impermeable or the inner impermeable lining remains robust.

From these results, we conclude that underground CAES in rock caverns with concrete linings at the comparatively shallow depth of 100 m is technically feasible. These findings will be further verified through ongoing pilot tests in Korea.

ACKNOWLEDGMENT

This research was supported by the Basic Research Project of the Korea Institute of Geosci-

ence and Mineral Resources (KIGAM, GP2012-001) funded by the Ministry of Knowledge and Economy of Korea. Funding from KIGAM for Dr. Jonny Rutqvist and Berkeley Lab was provided through the U.S. Department of Energy Contract No. DE-AC02-05CH11231.

REFERENCES

Hoseini M., V. Bindiganavile, N. Banthia, The effect of mechanical stress on permeability of concrete: A review. *Cement & Concrete Composites*, 31, 213–220, 2009.

Itasca, *FLAC3D, Fast Lagrangian Analysis of Continua in 3 Dimensions, Ver. 4.0* Minneapolis, Minnesota, 2009.

Kim, H.M., J. Rutqvist, D.W. Ryu, B.H. Choi, C. Sunwoo, W.K. Song, Exploring the concept of compressed air energy storage (CAES) in lined rock caverns at shallow depth: A modeling study of air tightness and energy balance, *Applied Energy*, 92, 653-667, 2012.

Pruess, K., C. Oldenburg, and G. Moridis, *TOUGH2 User's Guide, Version 2.0*, Report LBNL-43134, Lawrence Berkeley National Laboratory, Berkeley, Calif., 1999.

Rutqvist, J., Status of the TOUGH-FLAC simulator and recent applications related to coupled fluid flow and crustal deformations, *Comp. Geosci*., 37(6), 739-750, 2011.

Rutqvist, J., H.M. Kim, D.W. Ryu, J.H. Synn, W.K. Song, Modeling of coupled thermodynamic and geomechanical performance of underground compressed air energy storage in lined rock caverns, *Int. J. Rock Mech. Min. Sci*., 52, 71-81, 2012.